Contribution to finite element modelling of airfoil aeroelastic instabilities

J. Horáček[a,*], P. Sváček[b], M. Růžička[c], M. Feistauer[c]

[a] *Institute of Thermomechanics, Academy of Sciences of the Czech Republic, Dolejškova 5, 182 00 Praha 8, Czech Republic*
[b] *Czech Technical University Prague, Faculty of Mechanical Engineering, Karlovo nám. 13, 121 35 Praha 2, Czech Republic*
[c] *Charles University Prague, Faculty of Mathematics and Physics, Sokolovská 83, 186 75 Praha 8, Czech Republic*

Abstract

Nonlinear equations of motion for a flexibly supported rigid airfoil with additional degree of freedom for controlling of the profile motion by a trailing edge flap are derived for large vibration amplitudes. Preliminary results for numerical simulation of flow-induced airfoil vibrations in a laminar incompressible flow are presented for the NACA profile 0012 with three-degrees of freedom (vertical translation, rotation around the elastic axis and rotation of the flap). The developed numerical solution of the Navier – Stokes equations and the Arbitrary Eulerian-Lagrangian approach enable to consider the moving grid for the finite element modelling of the fluid flow around the oscillating airfoil. A sequence of numerical simulation examples is presented for Reynolds numbers up to about $\mathrm{Re} \approx 10^5$, when the system loses the aeroelastic stability, and when the large displacements of the profile and a post-critical behaviour of the system take place.
© 2007 University of West Bohemia. All rights reserved.

Keywords: flow – induced vibration, aeroelasticity, nonlinear vibrations, numerical simulations

1. Introduction

The contribution enlarges the previous studies of the authors [4] on finite element (FE) modelling of vibrations and aeroelastic instabilities of airfoils by including the additional degree of freedom for controlling of the profile motion by a trailing edge flap. The worked out method allows analyzing flow induced airfoil vibrations for various regimes, as, e.g. the flow of an isolated airfoil or an airfoil inserted into a wind tunnel. The presented computational results will demonstrate airfoil vibrations in dependence on time for various far field velocities and Reynolds numbers, the interaction of airflow and the airfoil for subcritical and supercritical regimes and the development of instabilities.

2. Description of the fluid flow and FE solution of Navier-Stokes equations

We assume that $(0, T)$ is a time interval and we denote by Ω_t a computational domain occupied by the fluid at time t. We denote by $\mathbf{u} = \mathbf{u}(x, t)$ and $p = p(x, t)$, $x \in \Omega_t$, $t \in (0, T)$ the flow velocity and the kinematic pressure (i.e. dynamic pressure divided by the density ρ of the fluid) and v denotes the kinematic viscosity. We have $\mathbf{u} = (u_1, u_2)$, where u_1 and u_2 are components of the velocity in the directions of the Cartesian coordinates x_1 and x_2 of x. By R and R^2 we denote the set of all real numbers and the set of all two-dimensional vectors, respectively.

---

[*] Corresponding author. Tel.:+420 266 053 125, e-mail: jaromirh@it.cas.cz.

In order to simulate flow in a moving domain, we employ the Arbitrary Eulerian-Lagrangian (ALE) method, based on an ALE mapping

$$A_t : \Omega_{ref} \rightarrow \Omega_t , \ X \rightarrow x(X,t) = A_t(X), \tag{1}$$

of the reference configuration $\Omega_{ref} = \Omega_0$ onto the current configuration Ω_t with the ALE velocity $\mathbf{w} = \partial A_t / \partial t$. We suppose that the ALE velocity at each point on the surface of the airfoil is equal to the velocity of its motion. By D^A / Dt we denote the ALE derivative – i.e. the derivative with respect to the reference configuration. In the domain Ω_t we consider the Navier-Stokes equations written in the following ALE form [3]:

$$\frac{D^A}{Dt} \mathbf{u} + \left[(\mathbf{u} - \mathbf{w}).\nabla \right] \mathbf{u} + \nabla p - \nu \ \Delta \mathbf{u} = 0 , \tag{2}$$

$$\nabla . \mathbf{u} = 0 , \tag{3}$$

to which we add the initial condition

$$\mathbf{u}(x,0) = \mathbf{u}_0 , \quad x \in \Omega_0 \tag{4}$$

and boundary conditions

$$\mathbf{u}\big|_{\Gamma_D} = \mathbf{u}_D , \qquad \mathbf{u}\big|_{\Gamma_{W_t}} = \mathbf{w}\big|_{\Gamma_{W_t}} , \qquad -p(p - p_{ref})\mathbf{n} + \nu \frac{\partial \mathbf{u}}{\partial \mathbf{n}} = 0 \quad \text{on} \ \ \Gamma_O . \tag{5}$$

Here $\mathbf{n}$ is the unit outer normal to the boundary $\partial \Omega_t$ of the domain Ω_t, Γ_D represents the inlet, Γ_0 is the outlet and Γ_{Wt} is the boundary of the airfoil at time t. Second condition represents the assumption that the fluid adheres to the airfoil. We denote by p_{ref} a prescribed reference outlet pressure. At the outlet we use here the boundary condition called the do-nothing condition [5].

The spatial semidiscretization of the Navier-Stokes equations written in the ALE form is performed by the stabilized finite element method [4]. In practical computations, the Taylor–Hood P2/P1 finite elements are used. The ALE time derivative is approximated by the second-order backward differentiation formula. The discrete Navier-Stokes problem is combined with the Runge-Kutta method for the solution of the nonlinear airfoil vibrations system.

3. Airfoil with three degrees of freedom

A solid flexibly supported airfoil with a control section is shown in Fig. 1, where the positions of the elastic axis (EO), and the position of the hinge (EF) of the control section are sketched. By h, α and β the plunging of the elastic axis, pitching of the airfoil and rotation of the flap are denoted, respectively, $\hat{\Delta}$ denotes the distance of the flap hinge from the elastic axis of the airfoil.

The elastic support of the airfoil is realized by translational and rotational springs. Kinetic and potential energy have to satisfy the Lagrange equations:

$$-\frac{d}{dt} \frac{\partial (E_\kappa - V)}{\partial \dot{q}_i} + \frac{\partial (E_\kappa - V)}{\partial q_i} + Q_i = 0, \tag{6}$$

where Q_i are generalized forces, E_k is the kinetic energy and V is the potential energy.

The potential energy V of the airfoil is given by

$$V = \frac{1}{2} k_{\alpha\alpha} \alpha^2 + \frac{1}{2} k_{\beta\beta} \beta^2 + \frac{1}{2} k_{hh} h^2 , \tag{7}$$

where $k_{\alpha\alpha}$, k_{hh}, $k_{\beta\beta}$ are the stiffness coefficients of the springs.

The airfoil in the neutral and deformed position is shown in Fig. 1. The horizontal displacement u and the vertical displacement w of any point on the airfoil chord can be expressed as

$$u = x - \min\left(x,\hat{\Delta}\right)\cos\alpha - \cos\left(\alpha+\beta\right)\left(x-\hat{\Delta}\right)^{+},$$

$$w = h + \min\left(x,\hat{\Delta}\right)\sin\alpha + \sin\left(\alpha+\beta\right)\left(x-\hat{\Delta}\right)^{+},$$

(8)

where $(\lambda)^{+}$ means the positive part of a number λ, i.e. $\lambda^{+} = \max(0, \lambda)$, and x denotes the local coordinate measured along the airfoil chord c from the elastic axis.
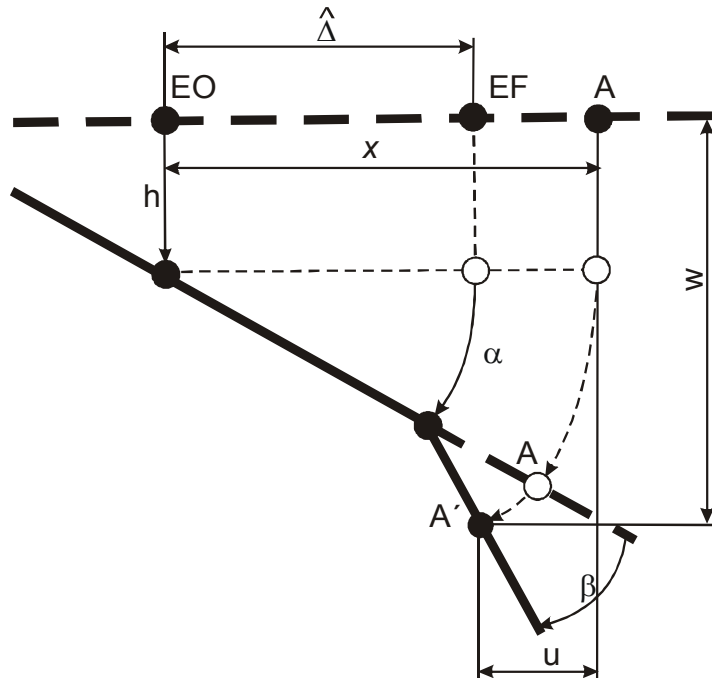

Fig. 1. Scheme of the airfoil with the flap.

3.1. Nonlinear equations of motion for large amplitudes

Using the nonlinear relations (4) for the displacements and dividing the airfoil chord c into the control section part c_2 and the main front part c_1, we have
on $c_1 : x < \hat{\Delta}$

$$u = x\left(1-\cos\alpha\right), \qquad w = h + x\sin\alpha,$$

and on $c_2 : x > \hat{\Delta}$

$$u = x - \hat{\Delta}\cos\alpha - \left(x-\hat{\Delta}\right)^{+}\cos\left(\alpha+\beta\right), \quad w = h + \hat{\Delta}\sin\alpha + \left(x-\hat{\Delta}\right)^{+}\sin\left(\alpha+\beta\right).$$

Let us divide the kinetic energy into three parts $E_k = E_1 + E_2 + E_3$ where,

$$E_1 = \int_{c_1}\frac{1}{2}\rho_s\left[\left(\frac{du}{dt}\right)^2 + \left(\frac{dw}{dt}\right)^2\right]dx, \quad E_2 = \int_{c_2}\frac{1}{2}\rho_s\left(\frac{du}{dt}\right)^2 dx, \quad E_3 = \int_{c_2}\frac{1}{2}\rho_s\left(\frac{dw}{dt}\right)^2 dx,$$

and where ρ_s is the airfoil material density.

First, consider the kinetic energy E_1:

$$E_1 = \int\limits_{x<\hat{\Delta}} \rho_s \frac{1}{2}\left[\left(\frac{du}{dt}\right)^2 + \left(\frac{dw}{dt}\right)^2\right] dx = \int\limits_{x<\hat{\Delta}} \rho_s \frac{1}{2}\left[x^2\dot{\alpha}^2 \sin^2\alpha + \left(x\dot{\alpha}\cos\alpha + \dot{h}\right)^2\right] dx =$$

$$= \frac{1}{2}\dot{\alpha}^2 I_1 + \frac{1}{2}\dot{h}^2 m_1 + \dot{\alpha}\dot{h}S_1\cos\alpha,$$

where $m_1 = \int\limits_{c_1} \rho_s(x)\,dx$, $I_1 = \int\limits_{c_1} x^2\rho_s(x)\,dx$ and $S_1 = \int\limits_{c_1} x\rho_s(x)\,dx$.

Further, for the kinetic energy E_2 we have

$$E_2 = \int\limits_{x>\hat{\Delta}} \rho_s \frac{1}{2}\left[\dot{\alpha}\hat{\Delta}\sin\alpha + \left(\dot{\alpha}+\dot{\beta}\right)\left(x-\hat{\Delta}\right)^+ \sin\left(\alpha+\beta\right)\right]^2 dx =$$

$$= \frac{1}{2}\hat{\Delta}^2 m_2\dot{\alpha}^2 \sin^2\alpha + \frac{1}{2}\left(\dot{\alpha}+\dot{\beta}\right)^2 \sin^2\left(\alpha+\beta\right)I_\beta + \dot{\alpha}\left(\dot{\alpha}+\dot{\beta}\right)\sin\alpha \sin\left(\alpha+\beta\right)\hat{\Delta}S_\beta,$$

where $m_2 = \int\limits_{c_2} \rho_s(x)\,dx$, $S_\beta = \int\limits_{c}\left(x-\hat{\Delta}\right)^+ \rho_s(x)\,dx$ is the static moment of the flap section

around the elastic axis of the control section EF, $I_\beta = \int\limits_{c}\left[\left(x-\hat{\Delta}\right)^+\right]^2 \rho_s(x)\,dx$ is the inertia

moment of the flap section around the elastic axis of the control section EF, and for the kinetic energy E_3 we have

$$E_3 = \int\limits_{x>\hat{\Delta}} \rho_s \frac{1}{2}\left[\dot{\alpha}\hat{\Delta}\cos\alpha + \left(\dot{\alpha}+\dot{\beta}\right)\left(x-\hat{\Delta}\right)^+ \cos\left(\alpha+\beta\right) + \dot{h}\right]^2 dx =$$

$$= \frac{1}{2}\hat{\Delta}^2 m_2\dot{\alpha}^2 \cos^2\alpha + \frac{1}{2}\left(\dot{\alpha}+\dot{\beta}\right)^2 \cos^2\left(\alpha+\beta\right)I_\beta + \frac{1}{2}m_2\dot{h}^2$$

$$+ \dot{\alpha}\left(\dot{\alpha}+\dot{\beta}\right)\cos\alpha \cos\left(\alpha+\beta\right)\hat{\Delta}S_\beta + m_2\hat{\Delta}\dot{\alpha}\dot{h}\cos\alpha + \dot{h}\left(\dot{\alpha}+\dot{\beta}\right)\cos\left(\alpha+\beta\right)S_\beta.$$

The following relations are introduced

$m = m_1 + m_2 = \int\limits_{c} \rho_s(x)\,dx$ … the total mass of the entire airfoil,

$S_\alpha = \int\limits_{c} x\rho_s(x)\,dx = S_1 + S_\beta + \hat{\Delta}\,m_2$ … the total static moment around the elastic axis EO,

$I_\alpha = \int\limits_{c} x^2\rho_s(x)\,dx = I_1 + I_\beta + 2\hat{\Delta}\,S_\beta + \hat{\Delta}^2\,m_2$ … the total inertia moment around the elastic axis,

$$\int\limits_{c} \rho_s x\left(x-\hat{\Delta}\right)^+ dx = I_\beta + \hat{\Delta}S_\beta,$$

$$\cos\beta = \cos\left(\left(\alpha+\beta\right)-\alpha\right) = \cos\alpha \cos\left(\alpha+\beta\right) + \sin\alpha \sin\left(\alpha+\beta\right)$$

and after summing up the energies E_1, E_2 and E_3 we get the kinetic energy

$$E_\kappa = \frac{1}{2}m\dot{h}^2 + \frac{1}{2}\dot{\alpha}^2\left(I_\alpha + 2\hat{\Delta}S_\beta\left(\cos\beta - 1\right)\right) + \frac{1}{2}\beta^2 I_\beta + \dot{\alpha}\dot{h}\left(S_\alpha\cos\alpha + S_\beta\left(\cos\left(\alpha+\beta\right)-\cos\alpha\right)\right) +$$

$$\dot{\alpha}\dot{\beta}\left(I_\beta + \hat{\Delta}S_\beta\cos\beta\right) + \dot{\beta}\dot{h}S_\beta\cos\left(\alpha+\beta\right).$$

Using the Lagrange equations, we find that

$$\frac{d}{dt}\left[m\dot{h}+\left(S_\alpha\cos\alpha+S_\beta\left(\cos(\alpha+\beta)-\cos\alpha\right)\right)\dot{\alpha}+\dot{\beta}S_\beta\cos(\alpha+\beta)\right]+k_{hh}h=0,$$

$$\frac{d}{dt}\left[\left(S_\alpha\cos\alpha+S_\beta\left(\cos(\alpha+\beta)-\cos\alpha\right)\right)\dot{h}+\left(I_\alpha+2\hat{\Delta}S_\beta\left(\cos\beta-1\right)\right)\dot{\alpha}+\left(I_\beta+\hat{\Delta}S_\beta\cos\beta\right)\dot{\beta}\right]$$

$$+\dot{\alpha}\dot{h}\left(S_\alpha\sin\alpha+S_\beta\left(\sin(\alpha+\beta)-\sin\alpha\right)\right)+\dot{\beta}\dot{h}S_\beta\sin(\alpha+\beta)+k_{\alpha\alpha}\alpha=0,$$

$$\frac{d}{dt}\left[S_\beta\cos(\alpha+\beta)\dot{h}+\left(I_\beta+\hat{\Delta}S_\beta\cos\beta\right)\dot{\alpha}+I_\beta\dot{\beta}\right]+\dot{\alpha}^2\hat{\Delta}S_\beta\sin\beta$$

$$+\dot{h}\left(\dot{\alpha}+\dot{\beta}\right)S_\beta\sin(\alpha+\beta)+\dot{\alpha}\dot{\beta}\hat{\Delta}S_\beta\sin\beta+k_{\beta\beta}\beta=0$$

and after differentiation with respect to time t we finally get

$$\left[m\ddot{h}+\left(S_\alpha\cos\alpha+S_\beta\left(\cos(\alpha+\beta)-\cos\alpha\right)\right)\ddot{\alpha}+S_\beta\cos(\alpha+\beta)\ddot{\beta}\right]+$$

$$+\dot{\alpha}^2\left(S_\beta-S_\alpha\right)\sin\alpha-\left(\dot{\alpha}+\dot{\beta}\right)^2S_\beta\sin(\alpha+\beta)+k_{hh}h=0,$$

$$\left(S_\alpha\cos\alpha+S_\beta\left(\cos(\alpha+\beta)-\cos\alpha\right)\right)\ddot{h}+\left(I_\alpha+2\hat{\Delta}S_\beta\left(\cos\beta-1\right)\right)\ddot{\alpha}+\tag{9}$$

$$+\left(I_\beta+\hat{\Delta}S_\beta\cos\beta\right)\ddot{\beta}+\left[-\hat{\Delta}S_\beta\dot{\beta}^2\sin\beta-2\hat{\Delta}S_\beta\dot{\alpha}\dot{\beta}\sin\beta\right]+k_{\alpha\alpha}\alpha=0,$$

$$S_\beta\cos(\alpha+\beta)\ddot{h}+\left(I_\beta+\hat{\Delta}S_\beta\cos\beta\right)\ddot{\alpha}+I_\beta\ddot{\beta}+\dot{\alpha}^2S_\beta\hat{\Delta}\sin\beta+k_{\beta\beta}\beta=0.$$

3.2. Linear equations of motion for small amplitudes

For small values of the angles α, β and of its derivatives $\dot{\alpha},\dot{\beta}$ (i.e. $\sin\alpha\approx\alpha$, $\sin\beta\approx\beta$, $\cos\alpha\approx1$, $\cos\beta\approx1$) the linearized equations reads

$$m\ddot{h}+S_\alpha\ddot{\alpha}+S_\beta\ddot{\beta}+k_{hh}h=0,$$

$$S_\alpha\ddot{h}+I_\alpha\ddot{\alpha}+\left(I_\beta+\hat{\Delta}S_\beta\right)\ddot{\beta}+k_{\alpha\alpha}\alpha=0,\tag{10}$$

$$S_\beta\ddot{h}+\left(I_\beta+\hat{\Delta}S_\beta\right)\ddot{\alpha}+I_\beta\ddot{\beta}+k_{\beta\beta}\beta=0.$$

3.3. Structural damping and aerodynamic forces loading the airfoil in viscous flow

After introducing the model of a proportional damping and the unsteady aerodynamic lift $L=L(t)$, aerodynamic moment $M=M(t)$ and hinge moment $M_\beta=M_\beta(t)$, the equations of motion for a flexibly supported rigid airfoil and small displacements read

$$\mathbf{M}\ddot{u}+\mathbf{B}\dot{u}+\mathbf{K}u=\mathbf{f},\tag{11}$$

where

$$\mathbf{M}=\begin{pmatrix}m & S_\alpha & S_\beta\\ S_\alpha & I_\alpha & \hat{\Delta}S_\beta+I_\beta\\ S_\beta & \hat{\Delta}S_\beta+I_\beta & I_\beta\end{pmatrix},\ \mathbf{K}=\begin{pmatrix}k_{hh} & 0 & 0\\ 0 & k_{\alpha\alpha} & 0\\ 0 & 0 & k_{\beta\beta}\end{pmatrix},\ \mathbf{B}=\begin{pmatrix}d_{hh} & 0 & 0\\ 0 & d_{\alpha\alpha} & 0\\ 0 & 0 & d_{\beta\beta}\end{pmatrix}$$

and $\mathbf{u}=(h,\ \alpha,\ \beta)^T$, $\mathbf{f}=(-L,\ M,\ M_\beta)^T$; $\mathbf{B}$ is the matrix modelling a viscous damping of the structure. In the case of large displacements, the damping and aerodynamic forces are added to the equations of motion for the airfoil (9) in a similar way.

The aerodynamic lift force L acting in the vertical direction and the torsional moments M and M_β are defined by

$$L = -l \int_{\Gamma_{w_t,airfoil}} \sum_{j=1}^{2} \tau_{2j} n_j dS, \quad M = +l \int_{\Gamma_{w_t,airfoil}} \sum_{i,j=1}^{2} \tau_{ij} n_j r_i^{ort} dS, \quad M_\beta = +l \int_{\Gamma_{w_t,flap}} \sum_{i,j=1}^{2} \tau_{ij} n_j r_i^{ort\,EF} dS,$$

(12)

where

$$\tau_{ij} = \rho \left[-p\delta_{ij} + \nu \left(\frac{\partial v_i}{\partial x_j} + \frac{\partial v_j}{\partial x_i} \right) \right],$$

(13)

$$r_1^{ort} = -(x_2 - x_{EO2}), \; r_2^{ort} = x_1 - x_{EO1}$$

and $\Gamma_{w_t,airfoil}$ is the surface of the whole airfoil. By τ_{ij} we denote the components of the stress tensor, v_1, v_2 are the velocity components in the directions x_1, x_2, p is the kinematic pressure, δ_{ij} denotes the Kronecker symbol, $\mathbf{n} = (n_1, n_2)$ is the unit outer normal pointing into the airfoil and $x_{EO} = (x_{EO1}, x_{EO2})$ is the position of the elastic axis (lying in the interior of the airfoil), $r_1^{ort\,EF} = -(x_2 - x_{EF2})$, $r_2^{ort\,EF} = x_1 - x_{EF1}$, l is the airfoil depth, and $\Gamma_{W_t,flap} \subset \Gamma_{W_t,airfoil}$ is the moving surface of the control section. Relations (12) and (13) define the coupling of the fluid and structural models.
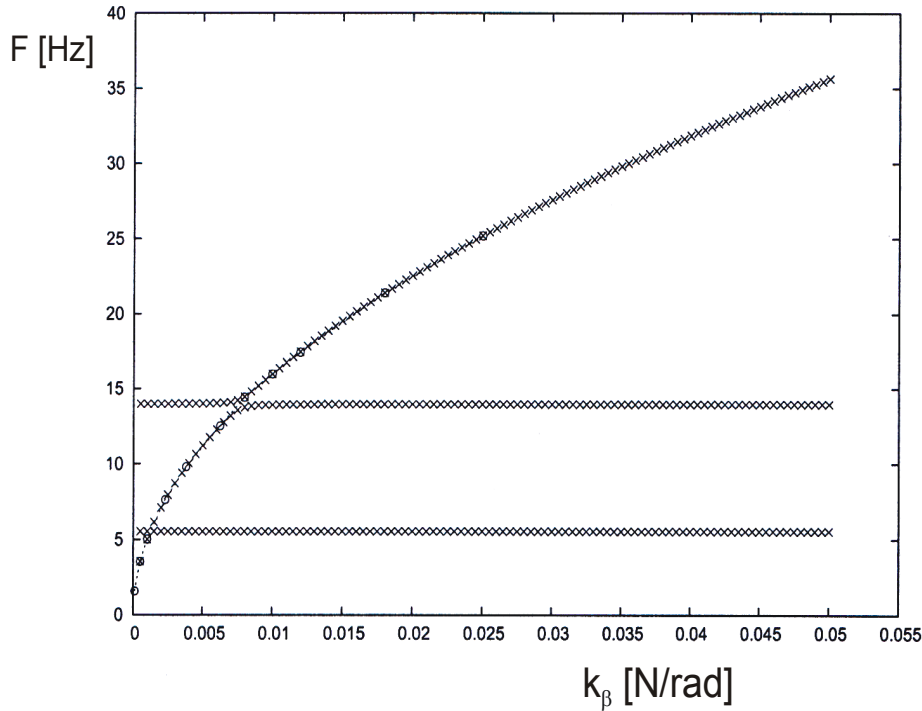

Fig. 2. Eigenfrequencies in dependence on flap stiffness.

3.4. Analysis of the eigenfrequencies for the structure in vacuo

The problem (10) was solved for zero aerodynamic forces ($\mathbf{f} = \mathbf{0}$) and

$$\mathbf{M} = \begin{pmatrix} 0.08662 & -0.7796 & S_\beta \\ -0.7796 & 4.87291.10^{-4} & \hat{\Delta} S_\beta + I_\beta \\ S_\beta & \hat{\Delta} S_\beta + I_\beta & I_\beta \end{pmatrix}, \quad \mathbf{K} = \begin{pmatrix} 105.109 & 0 & 0 \\ 0 & 3.695582 & 0 \\ 0 & 0 & k_{\beta\beta} \end{pmatrix},$$

where the stiffness $k_{\beta\beta} \in$ [0.001, 0.05] for the tensional spring of the flap was considered. Following the report [2], the input data for the flap were taken as follows: S_β = 0 kgm, I_β =1.10^{-6} kgm^2, $\hat{\Delta}$ =1.12 m. Influence of the proportional structural damping on eigenfrequencies was respected by a proportional damping **B** = 0.001 **K**.

Computed eigenfrequencies are shown in Fig. 4. The eigenfrequencies are in good agreement with the values in [2], denoted by small circles.

4. Aeroelastic simulations for small vibration amplitudes

The mesh, developed according to [1], and used for the FE computations is shown in Fig.7 for the profile NACA 0012 in two different positions during vibrations. The preliminary computations were performed for the airfoil with three degrees of freedom in viscous laminar flow, according to the method developed earlier for the profile with two degrees of freedom [4]. The input data were taken from the report [2], where the stiffness $k_{\beta\beta}$ = 0.05 N/rad was considered.

4.1. Examples of numerical simulations for linear structural model

The transient response of the structure for the profile rotation, the vertical displacement of the profile and the rotation of the flap was computed after releasing the profile motion from a small initial rotation angle α. The numerical simulations of the profile rotation α, the flap angle β and vertical displacement h of the elastic axis EO are shown in Figs. 4-6 for three far field flow velocities U_∞. If the simulations were performed for small velocities U_∞, when the profile motion is stable, i.e. when the vertical displacement and both rotation angles are decreasing in time.
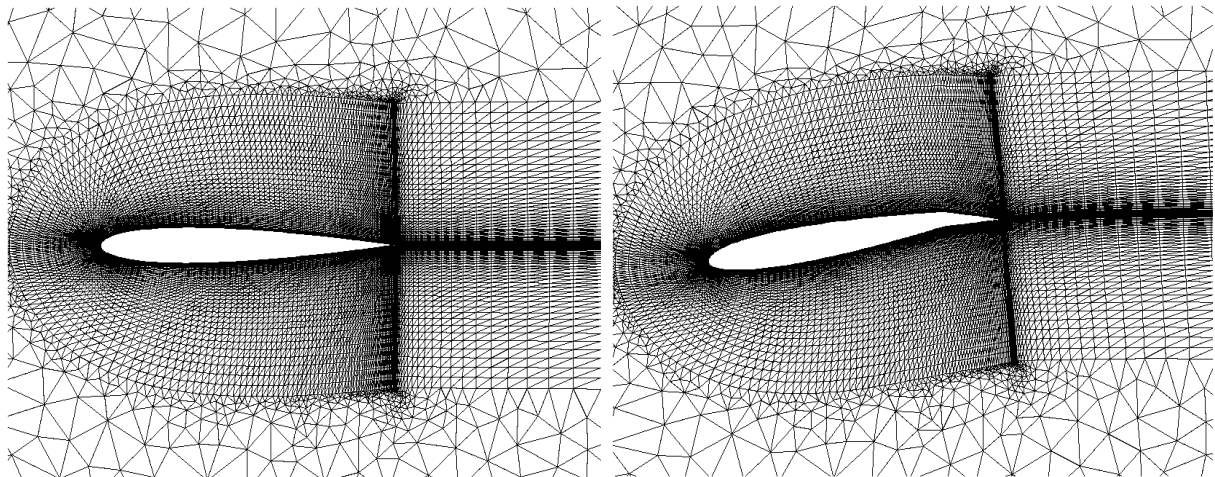

Fig. 3. Moving mesh around the vibrating profile with the flap in two different time instants.

Near the critical flow velocity the damping is reaching lower values and the decay of the vibration amplitudes is getting smaller – see Fig. 5. Above the critical flow velocity for flutter the amplitudes of vibration are growing in time very fast – see Fig. 6.

We note that according to the results of computations using NASTRAN code in [2] the system should lose the stability by flutter for the flow velocity U_∞ = 26.8 m/s.
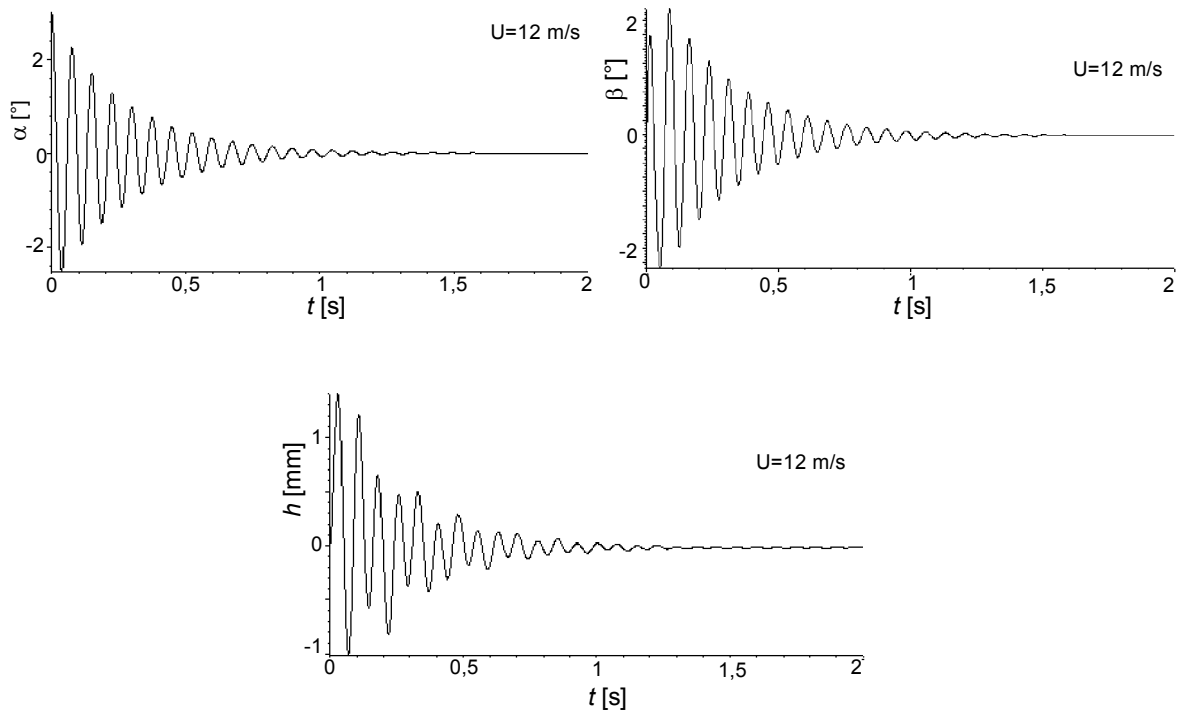
Fig. 4. Numerical simulations of the profile vibration for $U_\infty = 12$m/s.
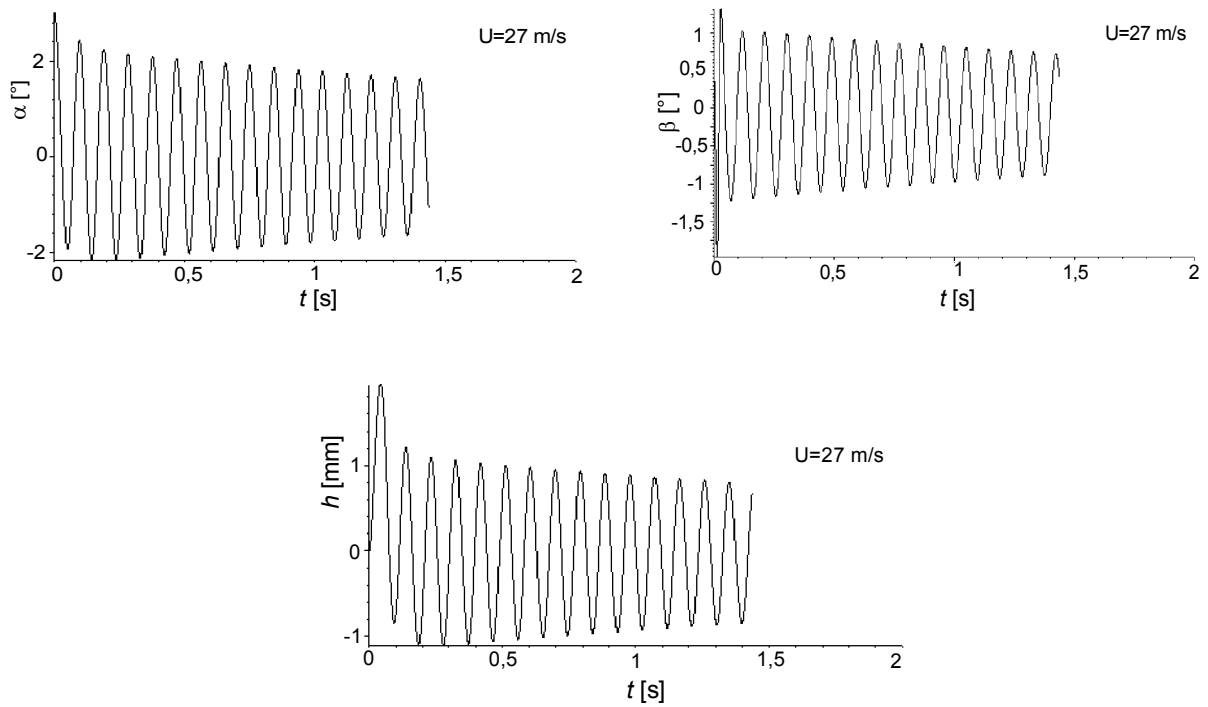

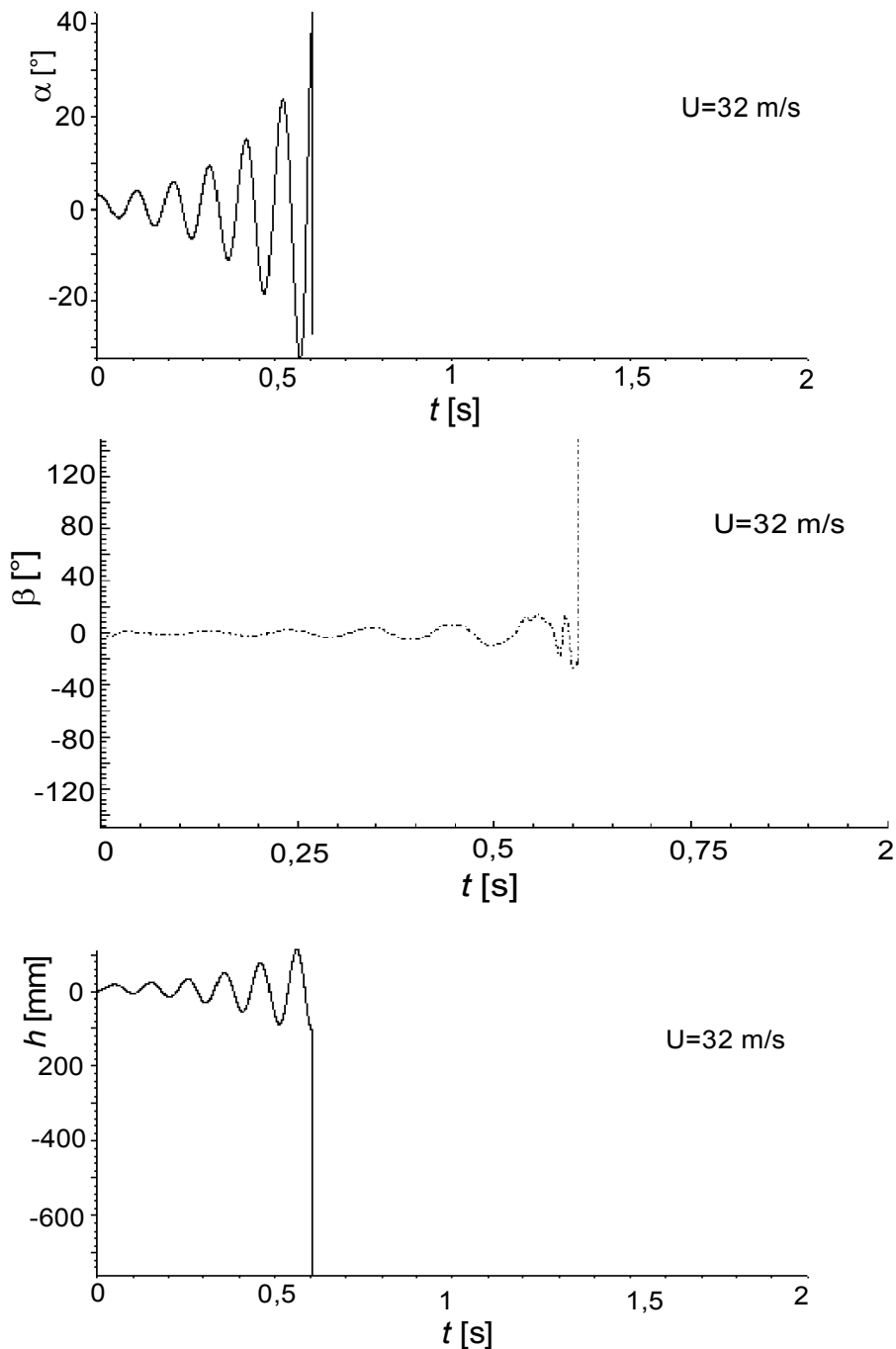Fig. 5. Numerical simulations of the profile vibration for $U_\infty = 27$m/s.

Fig. 6. Numerical simulations of the profile vibration for $U_\infty = 32$m/s.

5. Conclusion

We have been concerned with numerical simulation of flow induced airfoil vibrations of an airfoil with three degrees of freedom. The fluid flow is described by the Navier-Stokes equations for incompressible fluid in the ALE form, which allows taking into account time dependence of the computational domain for large deformations of the structure in post-critical regimes, when the aeroelastic system is unstable by flutter or divergence. The system of equations is discretized by a two step Backward Difference Formula in time and the FE

51

method in space stabilized by the Streamline – Upwind- Petrov – Galerkin method. The developed method is applied to the numerical simulation of interaction of a fluid and an airfoil for Reynolds numbers up to $\mathrm{Re} \approx 10^5$. The solution shows the robustness and applicability of the method to technically relevant situations.

Acknowledgments

References

[1] V. Dolejší, ANGENER V3.0. http://adel.karlin.mff.cuni.cz/~dolejsi/angen.htm.

[2] V. Losík, J. Čečrdle, Aeroelastic analysis of a verifying model of an airplane construction with three degrees of freedom - part I. Report No. V-1833/3210/05, VZLU (ARTI), Prague, 2005.

[3] T. Nomura, T.J.R Hughes, An arbitrary Lagrangian-Eulerian finite element method for interaction of fluid and a rigid body. Computer Methods in Applied Mechanics and Engineering 95 (1992) 115–138.

[4] P. Sváček, M. Feistauer, J. Horáček, Numerical simulation of flow induced airfoil vibrations with large amplitudes. Journal of Fluids and Structures 23 (2007) 391-412.

[5] S. Turek, Efficient Solvers for Incompressible Flow Problems: An Algorithmic and Computational Approach. Springer, Berlin, 1999.